ENERGETIC CATALYST-HYDROGEN PLASMA REACTION AS A POTENTIAL NEW ENERGY SOURCE

R. L. Mills, P. Ray, M. Nansteel, J. He, X. Chen, A. Voigt, and B. Dhandapani

BlackLight Power, Inc.
493 Old Trenton Road
Cranbury, NJ 08512

Introduction

A new chemically generated or assisted plasma source based on a resonant energy transfer mechanism (rt-plasma) has been developed that may be a new power source. One such source operates by incandescently heating a hydrogen dissociator and a catalyst to provide atomic hydrogen and gaseous catalyst, respectively, such that the catalyst reacts with the atomic hydrogen to produce a plasma. It was extraordinary that intense extreme ultraviolet (EUV) emission was observed by Mills et al.[1,2] at low temperatures (e.g. $\approx 10^3$ K) and an extraordinary low field strength of about 1–2 V/cm from atomic hydrogen and certain atomized elements or certain gaseous ions which singly or multiply ionize at integer multiples of the potential energy of atomic hydrogen, 27.2 eV. A number of independent experimental observations confirm that the rt-plasma is due to a novel reaction of atomic hydrogen which produces as chemical intermediates, hydrogen in fractional quantum states that are at lower energies than the traditional "ground" ($n = 1$) state. Power is released, and the final reaction products are novel hydride compounds or lower-energy molecular hydrogen as reported herein. The supporting data include EUV spectroscopy,[1–6,8–10] characteristic emission from catalysts and the hydride ion products,[2,6,9] lower-energy hydrogen emission,[3–5] chemically formed plasmas,[1,2,6,8,9] extraordinary (>100 eV) Balmer α line broadening,[1–3,6,7,9] population inversion of H lines,[9,10] elevated electron temperature,[7] anomalous plasma afterglow duration,[8] power generation,[3,4] and analysis of novel chemical compounds.[11]

The theory given previously[1,3–6,12] is based on applying Maxwell's equations to the Schrödinger equation. The familiar Rydberg equation (Eq. (1)) arises for the hydrogen excited states for n > 1 of Eq. (2).

$$E_n = -\frac{e^2}{n^2 8\pi\varepsilon_o a_H} = -\frac{13.598\,eV}{n^2} \tag{1}$$

$$n = 1,2,3,... \tag{2}$$

An additional result is that atomic hydrogen may undergo a catalytic reaction with certain atoms, excimers, and ions which provide a reaction with a net enthalpy of an integer multiple of the potential energy of atomic hydrogen, $m \cdot 27.2$ eV wherein m is an integer. The reaction involves a nonradiative energy transfer to form a hydrogen atom that is lower in energy than unreacted atomic hydrogen that corresponds to a fractional principal quantum number. That is

$$n = \frac{1}{2}, \frac{1}{3}, \frac{1}{4}, ..., \frac{1}{p}; \quad p \text{ is an integer} \tag{3}$$

replaces the well known parameter $n =$ integer in the Rydberg equation for hydrogen excited states. The $n = 1$ state of hydrogen and the $n = \frac{1}{\text{integer}}$ states of hydrogen are nonradiative, but a transition between two nonradiative states, say $n = 1$ to $n = 1/2$, is possible via a nonradiative energy transfer. Thus, a catalyst provides a net positive enthalpy of reaction of $m \cdot 27.2$ eV (i.e. it resonantly accepts the nonradiative energy transfer from hydrogen atoms and releases the energy to the surroundings to affect electronic transitions to fractional quantum energy levels). As a consequence of the nonradiative energy transfer, the hydrogen atom becomes unstable and emits further energy until it achieves a lower-energy nonradiative state having a principal energy level given by Eqs. (1) and (3). Processes such as hydrogen molecular bond formation that occur without photons and that require collisions are common. Also, some commercial phosphors are based on resonant nonradiative energy transfer involving multipole coupling.

Two H(1/p) atoms may react to form the corresponding molecule $H_2(1/p)$ that has a bond energy and vibrational levels that are p^2 times those of H_2 comprising uncatalyzed atomic hydrogen where p is an integer. The theory was given previously.[4,5,12] Since the υ = 0 to υ = 1 vibrational transition of H_2 is a resonant state of the corresponding transition of $H_2(1/2)$, emission due to the reaction $2H(1/2) \rightarrow H_2(1/2)$ is possible with vibronic coupling within the transition state at

$$E_{D+vib} = p^2 E_{D\,H_2} \pm \left(\frac{\upsilon^*}{3}\right) E_{vib\,H_2(\upsilon=0\rightarrow\upsilon=1)}, \quad \upsilon^* = 1,2,3... \tag{4}$$

where $E_{D\,H_2}$ and $E_{vib\,H_2(\upsilon=0\rightarrow\upsilon=1)}$ are the experimental bond and vibrational energies of H_2, respectively.

Atomic and molecular hydrogen are predicted to form stable states of lower energy than traditionally thought possible. Substantial spectroscopic and physical differences are anticipated. For example, novel EUV atomic and molecular spectral emission lines from transitions corresponding to energy levels given by Eqs. (1) and (3) and Eq. (4), respectively, are predicted. He^+ fulfills the catalyst criterion—a chemical or physical process with an enthalpy change equal to an integer multiple of 27.2 eV since it ionizes at 54.417 eV which is $2 \cdot 27.2$ eV. Thus, microwave discharges of helium–hydrogen mixtures were studied by EUV spectroscopy to search for line emission from transitions to fractional Rydberg states of atomic hydrogen and due to the formation of molecular hydrogen corresponding to fractional Rydberg states of atomic hydrogen. In addition, helium–hydrogen (90/10%) and helium–deuterium (90/10%) plasma gases were flowed through a high-vacuum (10^{-6} Torr) capable, liquid nitrogen cryotrap, and the condensed gas was characterized by gas chromatography (GC), mass spectroscopy (MS), visible and EUV optical emission spectroscopy (OES), and ^{1}H nuclear magnetic resonance (NMR) of the liquid-nitrogen-condensable gas dissolved in $CDCl_3$. Since the electronic transitions are very energetic, power balances were measured to determine whether this reaction has sufficient kinetics to merit its consideration as a practical power source.

Experimental

EUV spectroscopy was recorded on microwave discharge plasmas of hydrogen, nitrogen, oxygen, carbon dioxide, ammonia, helium, neon, argon, krypton, xenon, or 2% hydrogen mixed plasmas as well as nitrogen-methane (96/4%) according to the methods given previously.[3,4] Each ultrapure gas alone or mixture was flowed through a half inch diameter quartz tube at an inlet pressure of 1 Torr. The gas pressure to the cell was maintained during differential pumping by flowing the mixture while monitoring the pressure with a 10 Torr and 1000 Torr MKS Baratron absolute pressure gauge. The tube was fitted with an Opthos coaxial microwave cavity (Evenson cavity). The microwave generator was an Opthos model MPG-4M generator (Frequency: 2450 MHz). The input power to the plasma was set at 85 watts with forced air cooling of the cell. Extreme ultraviolet emission spectra were also obtained on these plasmas maintained in a glow discharge cell that comprised a five-

way stainless steel cross that served as the anode with a hollow stainless steel cathode according to the methods given previously.[5,7] For spectral measurement, the light emission was introduced to a normal incidence McPherson 0.2 meter monochromator (Model 302) equipped with a 1200 lines/mm holographic grating with a platinum coating. The wavelength region covered by the monochromator was 2–560 nm. The EUV spectrum was recorded with a channel electron multiplier (CEM) at 2500–3000 V or a photomultiplier tube (PMT) at -1000 V and a sodium salicylate scintillator. The wavelength resolution was about 0.2 nm (FWHM) with an entrance and exit slit width of $50\ \mu m$. The increment was 0.2 nm and the dwell time was 500 ms. The PMT (Model R1527P, Hamamatsu) used has a spectral response in the range of 185–680 nm with a peak efficiency at about 400 nm. The increment was 0.4 nm and the dwell time was 1 s. Peak assignments were based on a calibration against the known He I, He II, and Lyman series lines.

To achieve higher sensitivity at the shorter EUV wavelengths, the light emission was recorded with a McPherson 4° grazing incidence EUV spectrometer (Model 248/310G) equipped with a grating having 600 lines/mm with a radius of curvature of $\approx$ 1m. The angle of incidence was 87°. The wavelength region covered by the monochromator was 5–65 nm. The wavelength resolution was about 0.1 nm (FWHM) with an entrance and exit slit width of $300\ \mu m$. The increment was 0.1 nm and the dwell time was 500 ms. The light was detected by a CEM at 2400 V.

Condensable gas from helium–hydrogen (90/10%) microwave plasmas maintained in the Evenson cavity was collected in a high-vacuum (10^{-6} Torr) capable, liquid nitrogen cryotrap as described previously.[13] After each plasma run the cryotrap was pumped down to 10^{-5} Torr to remove any non-condensable gases in the system. The pressure was recorded as a function of time as the cryotrap was warmed to room temperature. Typically, about 3 Torr of condensed gas was collected in a 3 hr plasma run. Controls were hydrogen and helium alone.

The mass spectra ($m/e = 1$ to $m/e = 200$) of ultrahigh purity hydrogen (Praxair) control samples and samples of the condensable gas from the helium–hydrogen microwave plasmas were recorded with a residual gas analyzer. In addition, the ion current as a function of time of the mass to charge ratio of two ($m/e = 2$) was recorded while changing the electron gun energy from 30 to 70 to 100 eV for ultrapure hydrogen and the condensable gas from the helium–hydrogen plasma reaction.

Cryogenic gas chromatography was performed on a Hewlett Packard 5890 Series II gas chromatograph equipped with a thermal conductivity detector and a 60 meter, 0.32 mm ID fused silica Rt-Alumina PLOT column (Restek, Bellefonte, PA). The chromatographic column was submerged in liquid nitrogen, and samples were run at -196° C using Ne as the carrier gas.

OES was performed on the condensable gas from helium–hydrogen (90/10%) microwave plasmas to search for atomic hydrogen lines from plasma-decomposed $H_2(1/p)$. A sample tube was fitted with the Evenson cavity, and the visible spectrum was recorded during a discharge maintained at 80 W input power at about 2 Torr as described previously.[13]

EUV OES was performed on the condensable gas from helium–hydrogen (90/10%) and helium–deuterium (90/10%) microwave plasmas by flowing the gas through a needle valve from a gas collection tube to the half inch diameter quartz tube fitted with the Evenson cavity. The microwave system and EUV spectrometer was as given *supra.*, except that the differential pumping was enhanced using a 2 mm diameter pin-hole optic between the plasma tube and chamber, and only the turbo pump was used. With the typical pressure in the 20 cm^3 gas collection tube of 5–20 Torr, the plasma could be maintained for up to 30 minutes before the flowing gas was depleted. Peak assignments were based on a calibration against standard lines obtained before and after each run as given previously.[13]

Sealed ^1H NMR samples were prepared by collecting the condensed gas from the cryotrap in an NMR tube (5 mm OD, 23 cm length, Wilmad) which was then sealed as described previously.[13] Control NMR samples comprised ultrahigh purity hydrogen (Praxair) and the helium–hydrogen (90/10%) mixture with $CDCl_3$ solvent. The NMR spectra were recorded with a 300 MHz Bruker NMR spectrometer that was deuterium locked. The chemical shifts were referenced to the frequency of tetramethylsilane (TMS) at 0.00 ppm.

The excess power was measured by water bath calorimetry on helium–hydrogen (90/10%) plasmas maintained in a microwave discharge cell compared to control plasmas with the same input power. The water bath was calibrated by a high precision heater and power supply. A high precision linear response thermistor probe (Omega OL-703) recorded the temperature of the 45 L water bath as a function of time for the stirrer alone to establish the baseline. The heat capacity was determined for several input powers, 30, 40, and 50 W ± 0.01 W, and was found to be independent of input power over this power range within ± 0.05%. The temperature rise of the reservoir as a function of time gave a slope in °C/s. This slope was baseline corrected for the negligible stirrer power and loss to ambient. The constant known input power (J/s), was divided by this slope to give the heat capacity in J/°C. Then, in general, the total power output from the cell to the reservoir was determined by multiplying the heat capacity by the rate of temperature rise (°C/s) to give J/s.

Since the cell and water bath system were adiabatic, the general form of the power balance equation with the possibility of excess power is:

$$P_{in} + P_{ex} - P_{out} = 0 \tag{5}$$

where P_{in} is the microwave input power, P_{ex} is the excess power generated from the hydrogen catalysis reaction, and P_{out} is the thermal power loss from the cell to the water bath. Since the cell was surrounded by water that was contained in an insulated reservoir with negligible thermal losses, the temperature response of the thermistor T as a function of time t was determined to be

$$\dot{T}(t) = \left(1.907 \times 10^5\ \text{J/°C}\right)^{-1} \times P_{out} \tag{6}$$

where 1.907×10^5 J/°C is the heat capacity for the least square curve fit of the response to power input for the control experiments ($P_{ex} = 0$). The slope was recorded for about 2 hours after the cell had reached a thermal steady state, to achieve an accuracy of ± 1%.

Results and Discussion

The EUV emission was recorded from microwave and glow discharge plasmas of (1) hydrogen, helium, krypton, and xenon alone, and (2) krypton and xenon with 2% hydrogen over the wavelength range 5–125 nm. No peaks were observed in these controls except hydrogen peaks at wavelengths greater than about 80 nm for hydrogen alone or hydrogen mixed with krypton or xenon. Neither krypton or xenon satisfy the catalyst condition; thus, no novel lines were predicted. Similarly, only He I and He II peaks were observed for helium alone.

The EUV spectrum (5–100 nm) of the microwave cell emission of the helium–hydrogen (98/2%) mixture is shown in Figure 1.

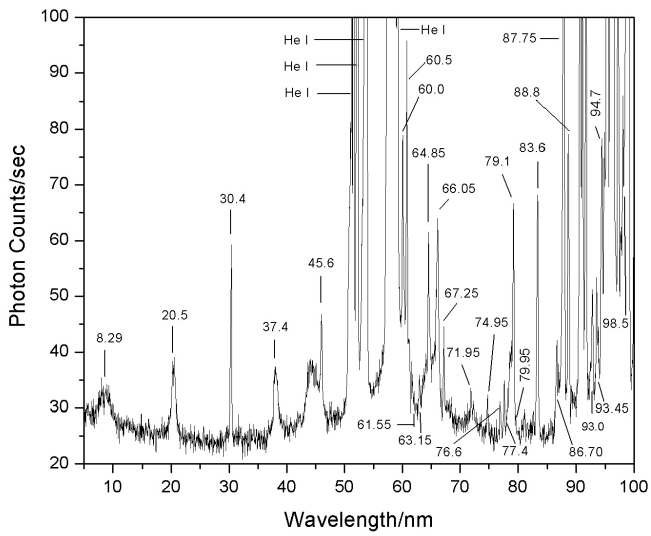

Figure 1. The EUV spectrum (5–100 nm) of the microwave cell emission of the helium–hydrogen (98/2%) mixture recorded with a normal incidence EUV spectrometer and a CEM. Reproducible novel emission lines were observed at 45.6 nm, 30.4 nm, and 8.29 nm with energies of $q \cdot 13.6$ eV where $q = 2$, 3, or 11 and at 37.4 nm and 20.5 nm with energies of $q \cdot 13.6$ eV where $q = 4$ or 6 that were inelastically scattered by helium atoms wherein 21.2 eV was absorbed in the excitation of He ($1s^2$) to He ($1s^12p^1$). In addition, a novel series of sharp wavelength-labeled peaks were observed in the 60–100 nm region that were assigned to members of peaks predicted at $E_{D+vib} = 17.913 \pm (\upsilon^*/3)\, 0.515902$ eV due to the reaction $2H(1/2) \rightarrow H_2(1/2)$ with vibronic coupling.

Reproducible novel emission lines were observed at 45.6 nm, 30.4 nm, and 8.29 nm with energies of $q \cdot 13.6\,\text{eV}$ where $q = 2,3,\text{or}\,11$ and at 37.4 nm, and 20.5 nm with energies of $q \cdot 13.6\,eV$ where $q = 4\,\text{or}\,6$ that were inelastically scattered by helium atoms wherein 21.2 eV was absorbed in the excitation of He ($1s^2$) to He ($1s^12p^1$) as discussed previously.[3,4,13] Additional spectra extended the series to $q = 1,2,3,4,6,7,8,9,\text{or}\,11$ as discussed before.[3,4,13] In addition, a series of peaks were observed in the 60–100 nm region of Figure 1. The wavelength-labeled peaks in Figure 1 match members of peaks predicted at $E_{D+vib} = 17.913 \pm \left(\frac{\upsilon^*}{3}\right) 0.515902\,eV$, $\upsilon^* = 1,2,3...$ due to the reaction $2H(1/2) \rightarrow H_2(1/2)$ with vibronic coupling. Hydrogen has no peaks below 80 nm. The peaks of the series also do not match helium as shown in control spectra and NIST tables[14] except for a distinguishable peak at 97.2 nm.[4] Figure 2 shows the plot of the theoretical emission vacuum wavelengths $E_{D\,H_2}$ due to the reaction $2H(1/2) \rightarrow H_2(1/2)$ with vibronic coupling at energies of $E_{D+vib} = p^2 E_{D\,H_2} \pm \left(\frac{\upsilon^*}{3}\right) E_{vib\,H_2(\upsilon=0\rightarrow\upsilon=1)}$ ($p = 2$) and the wavelengths observed over multiple spectra as partially shown in Figure 1. The data matched (Eq. (4)) to longer wavelengths for $\upsilon^* = 2$ to $\upsilon^* = 32$ and to shorter wavelengths for $\upsilon^* = 1$ to $\upsilon^* = 16$ to within the spectrometer resolution of about ± 0.05%.

Helium–hydrogen (90/10%) gas was flowed through the microwave tube and the cryosystem for 2 hours with the trap cooled to liquid nitrogen temperature. No change in pressure over time was observed when the dewar was removed, and the system was warmed to room temperature. The experiment was repeated under the same conditions but with a plasma maintained with 60 W forward microwave power and 10 W reflected. In contrast to the control case, a liquid-nitrogen-condensable gas was generated in the helium–hydrogen plasma reaction since the pressure due to the reaction product rose from 10^{-5} Torr to 3 Torr as the cryotrap warmed to room temperature.

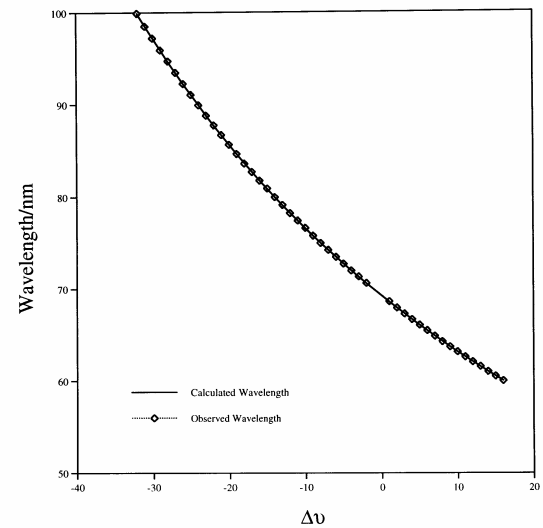

Figure 2. The plot of the theoretical (Eq. (4)) emission vacuum wavelengths E_{DH_2} due to the reaction $2H(1/2) \rightarrow H_2(1/2)$ with vibronic coupling at energies of $E_{D+vib} = p^2 E_{DH_2} \pm (\upsilon^*/3)\, E_{vib\,H_2}$ ($\upsilon=0 \rightarrow \upsilon=1$) ($p$=2) and the wavelengths observed such as those shown in Figure 1. The data matched to longer wavelengths for $\upsilon^* = 2$ to $\upsilon^* = 32$ and to shorter wavelengths for $\upsilon^* = 1$ to $\upsilon^* = 16$ to within the spectrometer resolution of about ± 0.05%.

The mass spectrum over the range $m/e = 1$ to $m/e = 200$ showed that the condensable gas was highly pure hydrogen. The $m/e = 2$ ion current as a function of time was recorded while changing the electron gun energy from 30 to 70 to 100 eV for ultrapure hydrogen and the condensed gas from the helium–hydrogen plasma reaction. The relative changes in the $m/e = 2$ ion current with increasing electron-beam energy indicated that the condensable gas has a higher ionization potential than ultrapure hydrogen. Upon increasing the ionization potential from 30 eV to 70 eV, the $m/e = 2$ ion current for the control hydrogen increased by a factor of about 30%; whereas, the gas collected under liquid nitrogen from the helium–hydrogen plasma increased by a factor of about 10 under the same pressure condition as that of the control.

The only known gases that show peaks on the liquid nitrogen-cooled Rt-Alumina PLOT column are helium and para-hydrogen and ortho-hydrogen, and these gases can be identified by their retention times of 13.7 min., 17.1 min., and 18.9 min., respectively. Trace helium (0.4%) and small peaks at the position of hydrogen were observed for the condensed gas that had the same 1:3 para-ortho ratio as H_2. However, two additional larger peaks were observed at 18.9 min. and 28.9 min. that had the same 1:3 relative ratio and were less thermally conductive than the neon carrier gas. The negative peaks could result from an on-column pressure change associated with the analyte gas.

With sufficient input power, the electrons at the tail of the Maxwellian distribution of a microwave plasma may be sufficiently energetic to ionize and decompose $H_2(1/2)$ (65 eV). The high resolution (± 0.1 nm) visible optical emission spectrum recorded on a

microwave discharge plasma of the liquid-nitrogen-condensable helium–hydrogen (90/10%) microwave discharge plasma gas showed strong Balmer α, β, γ, and δ lines of atomic hydrogen at 656.28 nm, 486.13 nm, 434.05 nm, and 410.17 nm, respectively, which indicated that the gas contained hydrogen.

The EUV optical emission spectra (45-100 nm) recorded on two separate microwave discharge plasmas of the liquid-nitrogen-condensable helium–hydrogen (90/10%) microwave discharge plasma gases collected over 48 hours are shown in Figure 3. A reproducible series of evenly spaced peaks were observed with a higher energy separation of 0.74 eV compared to the vibrational energy of H_2 ($E_{vib\,H_2(\upsilon=0\rightarrow\upsilon=1)} = 0.5159\,eV$) which is the highest known vibration transition energy. The series was similar to that shown in Figure 1, except that the energy spacing is about four times larger. Hydrogen has no emission below 80 nm. The peaks from the condensable gas did not match those of hydrogen for wavelengths >80 nm as well. The series of evenly spaced peaks did not match the He I and He II peaks observed from the helium gas discharge. The series of lines shown in Figure 3 was assigned to mixed vibration-rotational transitions of an electronically excited state of $H_2(1/p)$.

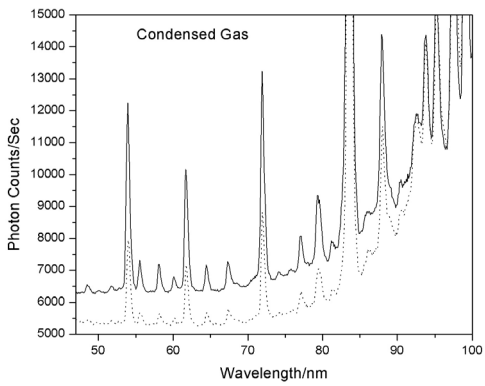

Figure 3. The EUV optical emission spectra (45–100 nm) recorded with a normal incidence EUV spectrometer and a CEM on two separate microwave discharge plasmas of the liquid-nitrogen-condensable helium–hydrogen (90/10%) microwave discharge plasma gases. A reproducible series of evenly spaced peaks were observed with a higher energy separation of 0.74 eV compared to the vibrational energy of H_2 ($E_{vib\ H_2}$ (υ=0 → υ=1) = 0.5159 eV) which is the highest known vibration transition energy. The series of lines was assigned to mixed vibration-rotational transitions of an electronically excited state of $H_2(1/p)$.

Deuterium substitution offers a method of definitively making the assignment of the condensed gas to a hydrogen-type molecule by the observation of a predicted shift of the spectral lines relative to the hydrogen spectrum. The EUV optical emission spectra (50-80 nm) recorded on microwave discharge plasmas of the liquid-nitrogen-condensable helium–hydrogen (90/10%) and helium–deuterium (90/10%) microwave discharge plasma gases are shown in Figure 4 (top) and (bottom), respectively. The isotope shift of the lines identified the series as belonging to $H_2(1/p)$ and supported the assignment of mixed vibration-rotational transitions of an electronically excited state of $H_2(1/p)$. The energy difference of 0.44 eV between the hydrogen and deuterium-based gases at 71.9 nm and 73.8 nm gives a good match to p=2 if anharmonicity and the increased electronic energy ΔE_{ele} of deuterium compared to hydrogen is considered as discussed previously.[13]

An exhaustive list of even remotely possible alternative assignments was considered for the EUV results for the reaction plasma EUV emission shown in Figure 1 and the liquid-nitrogen condensable H_2 shown in Figures 3 and 4. The only known species in a helium–hydrogen plasma, H^+, H_2^+, H_3^+, H^-, H, H_2, He_2^*, HeH^+, and remotely possibly HeH were eliminated since the spectra did not match or the species could not exist under the reaction conditions. Other exotic possibilities such as He_2^+, HHe_2^+, HHe_n^+ and He_n were eliminated due to the extremely specialized conditions required for their formation such as extremely low temperatures that were unlike those in the helium–hydrogen microwave plasmas.[15,16] Air contaminants were also eliminated. Emission from plasmas of nitrogen, oxygen, carbon dioxide, and ammonia or these gases with 2% hydrogen showed no emission in the region < 80 nm. In addition, water vapor present in the oxygen-hydrogen plasma showed no emission in this region. The spectrum of the nitrogen–methane (96/4%) plasma to form CN, C_x, and C_xH_y species (confirmed by visible spectra) showed no emission in this region. Emission of argon, krypton, and xenon as helium contaminants was eliminated. No emission was observed in the region <80 nm for krypton, krypton-hydrogen, xenon, xenon-hydrogen, and argon. Neon was eliminated based on spectral line mismatches and absences since only the Ne I lines were observed. Cl I, Br I, I I, and S I lines given by the NIST tables[14] were not detected in the visible or shorter wavelength regions. Silicon from the quartz tube wall was eliminated based on the NIST tables.[14] No pump contaminants were possible.

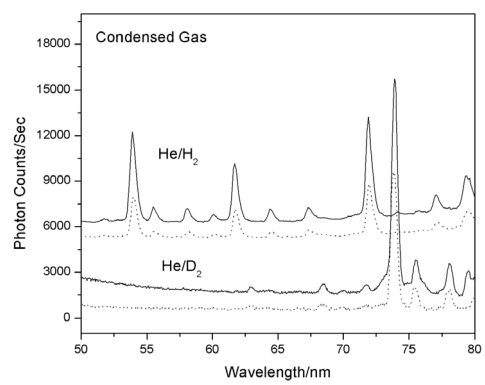

Figure 4. The EUV optical emission spectra (50–80 nm) recorded with a normal incidence EUV spectrometer and a CEM on two microwave discharge plasmas of the liquid-nitrogen-condensable helium–hydrogen (90/10%) (top) and helium–deuterium (90/10%) (bottom) microwave discharge plasma gases. The observation that the novel EUV emission spectrum shifted with deuterium substitution in a region where no hydrogen emission has ever been observed strongly supported the existence of lower-energy molecular hydrogen. The isotope shift of the lines also identified the series as belonging to mixed vibration-rotational transitions of an electronically excited state of $H_2(1/p)$.

^{1}H NMR spectra on sealed samples of condensable helium–hydrogen plasma gases dissolved in $CDCl_3$ relative to tetramethylsilane (TMS) are shown in Figure 5. Peaks observed in the 0 to 10 ppm region were a singlet peak at 7.26 ppm with side bands which matched $CDCl_3$ and two novel singlet peaks at 3.22 and 3.47 ppm. In addition, an H_2 peak was observed at 4.63 ppm. NMR chemical shifts of common laboratory solvents as trace impurities are given by Gottlieb et al.[17] All of the possible assignments were eliminated based on a mismatch between the observed and literature values for the chemical shifts, or in cases where the shifts matched to within ± 0.05 ppm, the known compound was eliminated based on a

mismatch between the multiplicity of the peak and/or the absence of other peaks of the known compound.

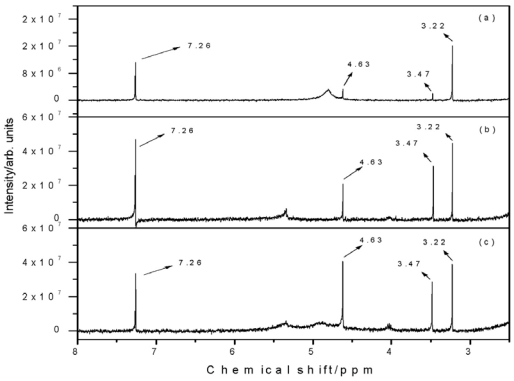

Figure 5. The ^{1}H NMR spectrum (2–7.5 ppm) on sealed samples of liquid-nitrogen-condensable helium–hydrogen plasma gases dissolved in $CDCl_3$ relative to tetramethylsilane (TMS). In each case, an H_2 peak was observed at 4.63 ppm. A singlet peak was observed at 7.26 ppm which matched $CHCl_3$. Two novel singlet peaks were observed at 3.22 ppm and 3.47 ppm which could not be assigned to a known compound. These upfield peaks relative to H_2 were assigned to $H_2(1/p)$ in two p quantum states.

The upfield peaks relative to H_2 only formed during the helium–hydrogen plasma reaction. The 3.22 ppm and 3.47 ppm peaks that could not be assigned to any known compound was assigned to $H_2(1/p)$ in two different quantum states. Even though the radii of corresponding states are related by inverse integers, the anticipated shifts are relatively small and matched those anticipated as discussed previously.[13] The assignments were further consistent with the EUV OES, GC, and MS results.

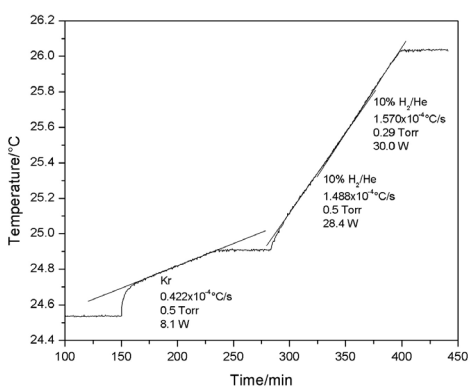

Figure 6. The *T(t)* water bath response to stirring and then with selected panel meter readings of the constant forward and reflected microwave input power to krypton was recorded. The microwave input power was determined to be 8.1 ± 1 W. A helium–hydrogen (90/10%) mixture was run at identical microwave input power readings as the control, and the excess power was determined to be 21.9 ± 1 W from the *T(t)* response.

The water bath calorimetry is an absolute standard and indicated $P_{in} = 8.1 \pm 1\,\mathrm{W}$ input power at the selected diode settings for all control plasmas. From these results, power input to the helium–hydrogen plasma was confidently known as the diode readings identically matched those of the controls. For example, the $T(t)$ water bath response to stirring and then with selected panel meter readings of the constant forward and reflected microwave input power to krypton was recorded as shown in Figure 6. Using the corresponding $\dot{T}(t)$ in Eq. (6), the microwave input power was determined to be 8.1 ± 1 W. A helium–hydrogen (90/10%) mixture was run at the same microwave input power readings as the control which corresponded to $P_{in} = 8.1 \pm 1\,W$ in Eq. (5). The $T(t)$ response was significantly increased for helium–hydrogen (90/10%) as shown in Figure 6. At 350 minutes, the pressure was changed from 0.5 Torr to 0.29 Torr. A slight increase in $\dot{T}(t)$ was observed at the lower pressure, possibly due to an increase in atomic hydrogen and He^+. The excess power was determined to be 21.9 ± 1 W from the corresponding $\dot{T}(t)$ using Eq. (6) and Eq. (5). The sources of error were the error in the calibration curve (± 0.05 W) and the measured microwave input power (± 1 W). The propagated error of the calibration and power measurements was ± 1 W. Given an excess power of 21.9 W in 3 cm^3 and a helium–hydrogen (90/10%) flow rate of 10.0 sccm, the excess power density and energy balance were high, 7.3 W/cm^3 and -2.9×10^4 kJ/mole H_2 (150 eV/H atom), respectively. The reaction of hydrogen to form water which releases -241.8 kJ/mole H_2 (1.48 eV/H atom) is about 100 times less than that observed. The results indicate that a new power source based on the catalysis of atomic hydrogen is not only possible, but is competitive with gas turbine combustion.

References

(1) Mills, R.L, Nansteel, M., Ray, P., *IEEE Trans. Plasma Sci.*, **2002**, *30* (2), 639.
(2) Mills, R.L, Nansteel, M., Ray, P., *New J. Phys*., **2002**, *4*, 70.1.
(3) Mills, R.L., Ray, P., Dhandapani, B, Nansteel, M., Chen, X., He, J., *J Mol. Struc*t., **2002**, *643* (1–3), 43.
(4) Mills, R.L., Ray, P., Dong, J., Nansteel, M., Dhandapani, B., He, J., *Vib. Spectrosc*., **2003**, *31* (2), 195.
(5) Mills, R.L., Ray, P., *Int. J. Hydrogen Energy,* **2002**, *27* (5), 533.
(6) Mills, R.L., Ray, P., *Int. J. Hydrogen Energy,* **2003**, *28* (8), 825.
(7) Mills, R.L., Ray, P., Dhandapani, B., Mayo, R.M., He, J., *J. Appl. Phys.*, **2002**, *92* (12), 7008.
(8) Conrads, H. Mills, R.L., Wrubel, Th., *Plasma Sources Sci. Technol*., in press.
(9) Mills, R.L., Ray, P., Mayo, R.M., *IEEE Trans. Plasma Sci*., **2003**, *31* (2), 236.
(10) Mills, R.L., Ray, P., Mayo, R.M., *Appl. Phys. Lett*., **2003**, *82* (11), 1679.
(11) Mills, R.L., Dhandapani, B, Nansteel, M., He, J., Shannon, T., Echezuria, A., *Int. J. Hydrogen Energy*, **2001**, *26* (4), 339.
(12) Mills, *The Grand Unified Theory of Classical Quantum Mechanics*, September 2001 Edition, BlackLight Power, Inc., Cranbury, New Jersey, Distributed by Amazon.com; January (2003) Edition posted at www.blacklightpower.com.
(13) Mills, R.L., Dhandapani, B, Nansteel, M., He, J., Ray, P., *J. Phys. Chem. B*, submitted.
(14) NIST Atomic Spectra Database, www.physics.nist.gov/cgi-bin/AtData/display.ksh.
(15) Baccarelli, I., Gianturco, F. A., Schneider, F., *J. Phys. Chem. A*, **1997**, *101*, 6054.
(16) Higgins, J., Callegari, C., Reho, J., Stienkemeier, F., Ernst, W.E., Gutowski, M., Scoles, G., *J. Phys. Chem. A*, **1998**, *102*, 4952.
(17) Gottlieb, H.E., Kotlyar, V., Nudelman, A., *J. Org. Chem.*, **1997**, *62*, 7512.